Journal Name

COMMUNICATION

A Twisted Macrocyclic Hexanuclear Palladium Complex with Internal Bulky Coordinating Ligands

Akira Nagai,[a] Takashi Nakamura[a] and Tatsuya Nabeshima*[a]

Received 00th January 20xx,
Accepted 00th January 20xx

DOI: 10.1039/x0xx00000x

www.rsc.org/

A macrocyclic hexanuclear palladium complex, which accumulates coordination sites on metals inside the cavity, was synthesized. The macrocycle was found to take a uniquely-twisted C_2-symmetric conformation when six molecules of a bulky pyridine derivative coordinated to the palladium.

The shape of macrocycles is a fundamental aspect that determines their properties such as molecular recognition.[1] Thus, it is important to create macrocycles with novel shapes and to control their conformations, so as to produce their unique functions.[2] Macrocycles have often been synthesized by the oligomerization of a single monomer for the sake of its simple preparation. Such cyclic oligomers are comprised of the same repeating unit, thus they usually have a high symmetry. In certain cases, however, the most stable conformation can be folded or twisted, which puts the monomeric units in different environments. The differentiated units can play distinctive roles in the resulting desymmetrized structures.[3,4] In this context, focusing on the dissymmetry of the macrocycles composed of the same repeating unit is an interesting approach to create elaborate functional molecules.

We now report a macrocyclic hexanuclear palladium complex, Pd-hexapap $[\mathbf{1}Pd_6L_6](BF_4)_6$ (L: exchangeable coordinating ligand), which accumulates coordination sites on metals inside the cavity. The macrocycle $[\mathbf{1}Pd_6L_6](BF_4)_6$ can bind up to six molecules via coordination bonds with the palladium at each Pd(pap) unit[5] (pap: 2-[(pyridin-2-ylmethylene)amino]phenol). Intriguingly, when bulky 4-*t*Bu-pyridine (tbp) ligands coordinate to the palladium, the resulting $[\mathbf{1}Pd_6(tbp)_6](BF_4)_6$ was found to take a uniquely-twisted C_2-symmetric conformation with three different $[Pd(pap)(tbp)]^+$ units (Fig. 1a).

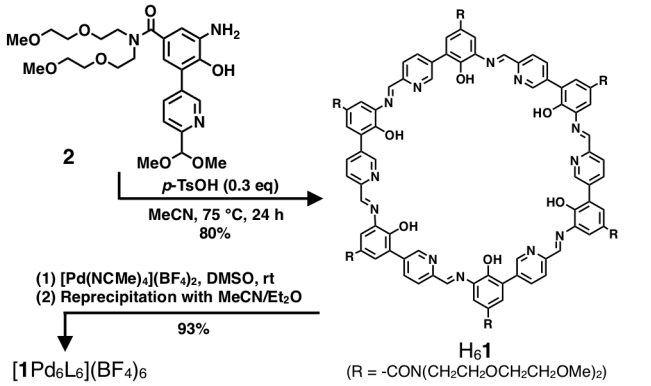

Scheme 1. Synthesis of macrocyclic ligand hexapap $H_6\mathbf{1}$ from bifunctional monomer **2**, and synthesis of Pd-hexapap complex $[\mathbf{1}Pd_6L_6](BF_4)_6$ (L = MeCN, H_2O, and Et_2O).

We have previously reported a macrocyclic hexapap ligand with a *t*Bu substituent at each pap unit.[4] However, its solubility in common organic solvents is low due to the structure in which many aromatic rings are consecutively arranged. To overcome this problem, we designed a novel hexapap ligand $H_6\mathbf{1}$ possessing the *N*,*N*-bis[2-(2-methoxyethoxy)ethyl]amide group (Scheme 1). $H_6\mathbf{1}$ was synthesized by hexamerization of the bifunctional monomer **2** that has both the 2-aminophenol unit and acetal-protected 2-formylpyridine unit (see ESI for the synthesis of **2**). The protection of the formyl group made the isolation of **2** possible by preventing self-oligomerization. The synthetic condition for the macrocyclization was optimized, and $H_6\mathbf{1}$ was obtained in 80% yield by heating the monomer **2** at 75 °C in MeCN in the presence of 0.3 equiv. of *p*-TsOH. The deprotection of the formyl group and Schiff-base formation proceeded in one pot. The macrocyclic ligand $H_6\mathbf{1}$ was characterized by ^1H NMR, MALDI TOF-MS, IR, and elemental analysis (see ESI). In the ^1H NMR spectrum (Fig. S13), a set of signals corresponding to one pap unit was observed, which demonstrates its time-averaged six-fold symmetry as well as its purity. The MALDI TOF mass spectrum showed strong peaks at m/z = 2682 with the isotropic distribution matching $[H_6\mathbf{1}\cdot Na]^+$, thus supporting the selective formation of the cyclic hexamer

[a] *Graduate School of Pure and Applied Sciences and Tsukuba Research Center for Energy Materials Science (TREMS), University of Tsukuba, 1-1-1 Tennodai, Tsukuba, Ibaraki 305-8571, Japan. E-mail: nabesima@chem.tsukuba.ac.jp*
Electronic Supplementary Information (ESI) available: Detailed synthetic procedures, characterization data, photophysical measurements, and crystallographic files (CIF). CCDC 1881523. See DOI: 10.1039/x0xx00000x

over the other linear or cyclic oligomers (Figs. S14, S15). By virtue of the 2-(2-methoxyethoxy)ethyl chains, H_6**1** has a good solubility (> 5 mg / mL) in organic solvents such as CH_2Cl_2, $CHCl_3$, DMF, and DMSO.

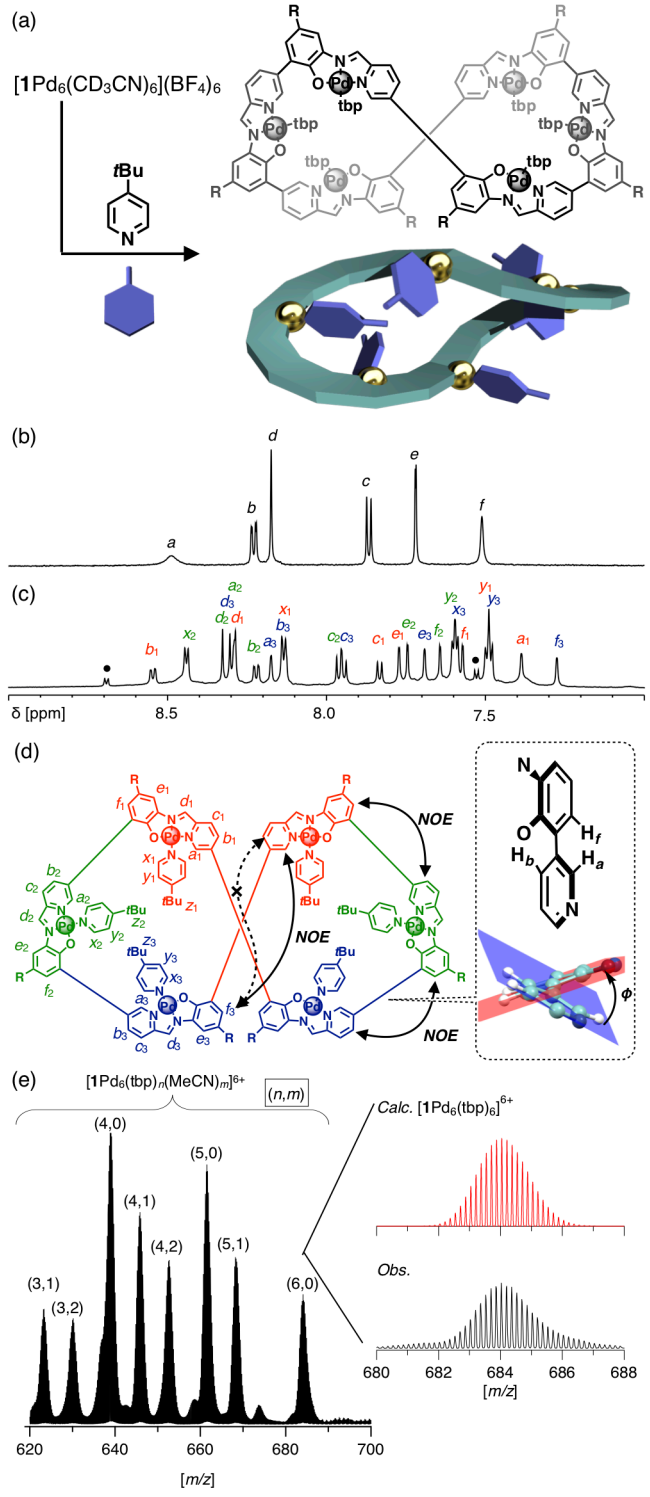

Figure 1. Metallomacrocycle [**1**$Pd_6(tbp)_6$]$(BF_4)_6$ (tbp: 4-*tert*-butylpyridine) and its twisted structure. (a) [**1**$Pd_6(tbp)_6$]$(BF_4)_6$ prepared by binding tbp to the inward coordination sites of Pd-hexapap [**1**Pd_6L_6]$(BF_4)_6$. R = -CON($CH_2CH_2OCH_2CH_2OMe$)$_2$. (b, c) ^{1}H NMR spectra (600 MHz, CD_3CN, 3 mM). (b) Pd-hexapap [**1**Pd_6L_6]$(BF_4)_6$ (L = solvent). (c) [**1**$Pd_6(tbp)_6$]$(BF_4)_6$. Filled circles indicate signal of [Pd(tbp)$_4$]$(BF_4)_2$ (d) Chemical structure of [**1**$Pd_6(tbp)_6$]$^{6+}$ and assignment of ^{1}H NMR signals. The structure is colored to show the C_2 symmetry of the entire structure. Double-headed arrows indicate the pairs of ^{1}H–^{1}H between which the NOE cross peaks were observed (Fig. S35). (Inset) dihedral angle ϕ between adjacent pap units. (e) ESI TOF mass spectrum of [**1**$Pd_6(tbp)_6$] $(BF_4)_6$ (positive, MeCN, 5 μM). (*n*,*m*) on each signal indicate the numbers of coordinating tbp (*n*) and MeCN (*m*) ligands, respectively. The simulated and observed isotope patterns of [**1**$Pd_6(tbp)_6$]$^{6+}$ are shown in the inset.

The hexanuclear palladium complex [**1**Pd_6L_6]$(BF_4)_6$ was synthesized by mixing the ligand H_6**1** and [Pd(NCMe)$_4$]$(BF_4)_2$ in DMSO. After the reaction, DMSO and other volatiles were removed under reduced pressure, and the residue was reprecipitated from MeCN/Et_2O. The obtained complex was characterized by ^{1}H, ^{11}B, ^{19}F NMR, ESI-TOF MS, UV-vis, IR, and elemental analysis (see ESI). The ^{1}H NMR spectrum of [**1**Pd_6L_6]$(BF_4)_6$ in CD_3CN at 298 K shows its time-averaged six-fold symmetry (Fig. 1b). In acetonitrile, which is a good coordinating solvent, the majority of the coordinating ligand of [**1**Pd_6L_6]$(BF_4)_6$ is speculated to be MeCN, indicated by the ESI-TOF MS measurement (Fig. S18–S21). The metal-free ligand H_6**1** has an absorption at 392 nm (ε = 1.1 × 10^5 $cm^{-1}\cdot M^{-1}$, $CHCl_3/CH_3OH$ = 10/1, 4.8 μM), while the palladium complex [**1**Pd_6L_6]$(BF_4)_6$ exhibited its absorption in the visible region at 572 nm (ε = 5 × 10^4 $cm^{-1}\cdot M^{-1}$, MeCN, 7.1 μM) (Fig. S25). A TD-DFT calculation suggested that the visible absorption of the palladium complex originated from a charge-transfer transition within the Pd(pap) moiety (Fig. S31).

In order to obtain more-detailed structural information about the Pd-hexapap macrocycle, the ^{1}H-^{1}H NOESY spectrum of [**1**Pd_6L_6]$(BF_4)_6$ in CD_3CN was measured (Fig. S17). Focusing on the NOE between the Pd(pap) units, the proton *f* (5th position of the 2-aminophenol unit) showed correlations with both the proton *b* (4th position of the 2-formylpyridine unit) and the proton *a* (6th position of the 2-formylpyridine unit). This result implies that the relative orientations between the Pd(pap) units may vary in the macrocyclic structure. We also synthesized a Zn-hexapap complex [**1**$Zn_6(acac)_6$] ($acac^-$: acetylacetonate) from the ligand H_6**1** and Zn(acac)$_2$ salt under similar conditions to synthesize the Zn-hexapap with the *t*Bu substituent[4] (see ESI). In contrast to the palladium complex, the NOESY measurement of [**1**$Zn_6(acac)_6$] gave NOE correlations between protons *f* and *b*, but did not give correlations between *f* and *a* (Fig. S24). This suggests that the Pd-hexapap [**1**Pd_6L_6]$(BF_4)_6$ takes a different conformation from the Zn-hexapap [**1**$Zn_6(acac)_6$].

Next, we investigated the ligand exchange reaction of the macrocycle inside the cavity. Intriguingly, the formation of a single species with a lower symmetry was suggested from the ^{1}H NMR when 6 equiv. of 4-*t*Bu-pyridine (tbp) reacted with [**1**Pd_6L_6]$(BF_4)_6$ (L: solvent) in CD_3CN (Fig. 1c). ESI TOF mass measurements of the diluted MeCN solution of this sample showed a set of signals assigned to [**1**$Pd_6(tbp)_n(MeCN)_m$]$^{6+}$ ($(n + m) \leqq 6$) (Fig. 1e). The species with the largest molecular weight was [**1**$Pd_6(tbp)_6$]$(BF_4)_6$, which suggested the coordination of the tbp ligand to each Pd(pap)unit. In the ^{1}H NMR spectrum, three different [Pd(pap)(tbp)]$^+$ units were observed. Based on the ^{1}H-^{1}H COSY, NOESY, and ROESY measurements, all the ^{1}H NMR signals of [**1**$Pd_6(tbp)_6$]$(BF_4)_6$ were successfully assigned (Fig. 1c, Figs. S34 and S35, Tables S1 and S2). NOE correlations between the [Pd(pap)(tbp)]$^+$ units gave important information about the

conformation of the macrocyclic framework. Focusing on the correlations between the protons of adjacent units, (*f*, *a*) and (*f*, *b*), the arrangement of three different [Pd(pap)(tbp)]$^+$ units was determined to be in the order of 1,2,3,1,2,3 (1 (red), 2 (green), and 3 (blue), see assignments and coloring for Fig. 1d). NOE between units (1,2) and (2,3) were observed for protons *f* and *b*. Both protons were positioned outside with respect to the palladium center, thus this part of the macrocycle is curved with the palladium centers inward. On the other hand, the NOE between units (3,1) were observed for protons *f* and *a*. Thus, the relative orientation between the [Pd(pap)(tbp)]$^+$ units is reversed at this point.

Despite many trials, we were unable to obtain a single crystal of [**1**Pd$_6$(tbp)$_6$](BF$_4$)$_6$ for X-ray crystallography analysis, so we investigated the structure by molecular mechanics (MM) calculations. The energy-minimized structure of [**1**´Pd$_6$(tbp)$_6$]$^{6+}$ obtained by MM calculations is consistent with the observation by the 2D NMR (Fig. 2, see ESI for the calculation details) (**1**´$^{6-}$: R = H in the structure of **1**$^{6-}$). The overall structure roughly belongs to the C_2 point group symmetry. Three different [Pd(pap)(tbp)]$^+$ units exist, which are consistent with the ^{1}H NMR observation. Each Pd(pap) unit is relatively planar. Meanwhile, the relative configurations of the adjacent units are not coplanar. The dihedral angle ϕ between the two least square planes of the benzene and pyridine rings of the adjacent pap units is a good indicator of the macrocyclic conformation (Fig. 1d). The three respective dihedral angles ϕ in the calculated approximate C_2-symmetric structure of [**1**´Pd$_6$(tbp)$_6$]$^{6+}$ are –54, –50, and 134° (averaged values of the corresponding diagonal units), which represent its large twist. In this calculated structure, the distances *d* between the protons pairs (f_1, b_2), (f_2, b_3), and (f_3, a_1) (see Fig. 1d), which are variable depending on the dihedral angle ϕ, are 2.61 , 2.57, and 2.54 Å, respectively (averaged values). The same distances *d* of [**1**Pd$_6$(tbp)$_6$](BF$_4$)$_6$ in CD$_3$CN were estimated from the intensity of the NOE between the corresponding protons, and were found to be 2.58, 2.60, and 2.60 Å, respectively (Table S3). Thus, the values in the modeling matched well with those evaluated from the NOE, which supports the C_2-symmetric structure obtained by the MM calculation.

The size of the tbp ligand is too large to be simply accumulated inside the cavity. Two of the tbp ligands (unit 2, green in Figs. 1 and 2) are directed toward the central cavity of the macrocycle. Meanwhile, the other two tbps (unit 1, red) are directed out toward one face of the macrocycle, and the two remaining tbps (unit 3, blue) are directed to the opposite face (Figs. 2b and 2c). The dense packing and steric hindrance in [**1**Pd$_6$(tbp)$_6$]$^{6+}$ are the contributing factors that led to the slower structural conversion. A detailed investigation of the chemical shift values revealed that a_1 was the proton signal that has the largest upfield shift upon the formation of [**1**Pd$_6$(tbp)$_6$](BF$_4$)$_6$ from [**1**Pd$_6$(CD$_3$CN)$_6$](BF$_4$)$_6$ (from 8.51 to 7.39 ppm, Table S1). This upfield shift was explained by the shielding effect from the adjacent amino-phenol ring (unit 3) as well as from the tbp ligand (unit 1). On the other hand, the proton experiencing the largest downfield shift upon tbp binding was b_1 (from 8.25 to 8.55 ppm, Table S1). This proton b_1 was positioned at the Pd(pap) connection point in which the orientation was reversed. The other comparison of the chemical shift changes is consistent with the proposed C_2-symmetric twisted structure. The support for the calculated structure was further provided by the ^{1}H-^{1}H ROESY measurement (Fig. 2a). Several clear ROE correlations were observed between the *t*Bu protons of the tbp ligand of unit 2 (green) and pap protons of unit 1 (red), and the distances between these proton pairs are 3.0–4.9 Å in the calculated structure (Fig. 2d). The other interunit ROEs also support the optimized structure (Fig. 2e).

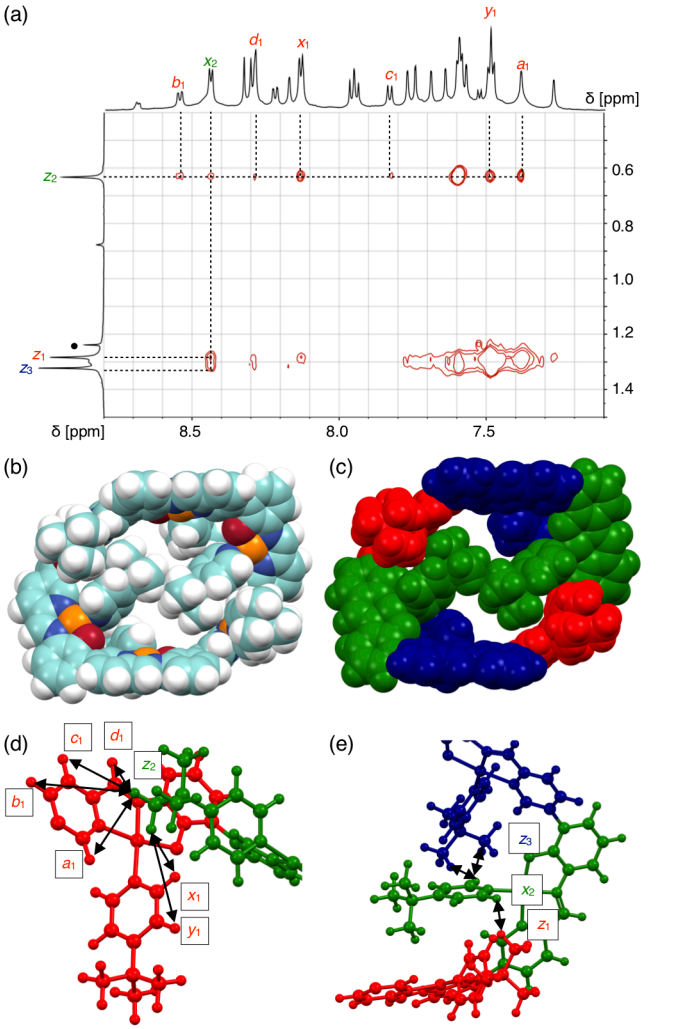

Figure 2. The structure of C_2-symmetric twisted metallomacrocycle [**1**Pd$_6$(tbp)$_6$](BF$_4$)$_6$ (tbp: 4-*tert*-butylpyridine). See also Figures 1c and 1d for the assignments of the ^{1}H NMR signals and the coloring. (a) ^{1}H–^{1}H ROESY spectrum of [**1**Pd$_6$(tbp)$_6$](BF$_4$)$_6$ (600 MHz, CD$_3$CN, 6 mM (saturated)). (b–e) The structure of [**1**´Pd$_6$(tbp)$_6$]$^{6+}$ obtained by molecular mechanics calculations (see ESI for details). H$_6$**1**´: R = H in the structure of H$_6$**1**. (b, c) A space-filling model. (b) A model colored according to the elements. C, light green; N, blue; O, red; H, white; Pd, orange. (c) A model colored to show the pseudo C_2 symmetry of the entire structure. (d, e) Pairs of ^{1}H-^{1}H atoms between which cross peaks were observed in the ROESY spectrum.

As for possible conformations of [**1**Pd$_6$(tbp)$_6$]$^{6+}$ other than the C_2-symmetric twisted structure, a C_6-symmetric planar conformation is unstable because the dihedral angle ϕ between the pap units cannot take 0° due to the steric repulsion of the *o*-phenoxy group with the adjacent pyridine ring. The energy-minimized structure of a C_i-symmetric conformation, which can

be regarded as a distorted S_6-symmetric conformation (up-down-up-down-up-down relations for six $[Pd(pap)(tbp)]^+$), has a calculated energy higher than the C_2-symmetric conformer (+38 kJ/mol) (Fig. S36). This C_i-symmetric conformation is ruled out based on the NOE pattern between the pap units (Fig. 1d), the ROEs between tbp and pap units (Fig. 2d), and the absence of chemical exchange between the three different pap units during the NOESY mixing time (0.3 s).

The bulkiness of the tbp ligand is a contributing factor to the successful observation of the C_2-symmetric twisted structure. Upon reacting the unsubstituted pyridine (py) with the $[\mathbf{1}Pd_6L_6](BF_4)_6$ (L: solvent) in CD_3CN, the coordination of pyridine at the internal coordination sites occurred, and the formation of $[\mathbf{1}Pd_6(py)_6](BF_4)_6$ was confirmed by ^{1}H NMR and ESI-MS (Figs. S37–S40, Table S4). The ^{1}H NMR spectrum of $[\mathbf{1}Pd_6(py)_6](BF_4)_6$ in CD_3CN suggests its time averaged six-fold symmetry, which suggests its flexible structure. Thus, the steric factor of the internally bound ligands significantly affects the structural mobility of the macrocyclic framework.

The complex $[\mathbf{1}Pd_6(tbp)_6]^{6+}$ has the C_2-symmetric point group symmetry, thus is inherently chiral. To investigate the interaction with external molecules utilizing the twisted chiral structure, the reaction of the Δ-TRISPHAT tetrabutylammonium salt (1 eq),[6] a chiral anion with a rigid structure, with $[\mathbf{1}Pd_6(tbp)_6](BF_4)_6$ (3 mM) was studied in CD_3CN. As a result, the ^{1}H NMR signals of the complex split into two sets with the integral ratio of 6:4 (Figs. S41 and S42). This suggests the formation of two diastereomeric ion pairs between $[\mathbf{1}Pd_6(tbp)_6]^{6+}$ and $(\Delta\text{-TRISPHAT})^-$, and one diastereomer existed in excess over the other. Furthermore, upon measuring the circular dichroism spectrum of the solution of $[\mathbf{1}Pd_6(tbp)_6]^{6+}\bullet(\Delta\text{-TRISPHAT})^-$, a negative Cotton effect was observed around 560 nm (CT band of Pd(pap) unit) (Fig. S43). The response presumably results from the twisted hexameric Pd(pap) macrocycle. Hence, the Pd-hexapap has a significant potential as chiroptical sensors that recognize chiral substrates by direct (= coordinative) and indirect (= electrostatic) bindings.

To summarize, we synthesized the novel macrocyclic hexanuclear palladium complex $[\mathbf{1}Pd_6L_6](BF_4)_6$ (L: exchangeable coordinating ligand), which accumulates coordination sites of metals in the cavity. The binding of six molecules of bulky tbp ligands in the cavity led to the formation of the uniquely twisted $[\mathbf{1}Pd_6(tbp)_6](BF_4)_6$ complex. The new metallomacrocycle is endowed with the appropriate rigidity and flexibility, thus is promising as an allosteric host that can amplify a slight structural difference in the effector. Furthermore, the internal space surrounded by exchangeable coordination sites can be utilized for capture of the substrate[7] and/or catalytic sites[8] via a multipoint metal-ligand coordination, and such applications are now being investigated.

This work was supported by JSPS KAKENHI Grant Numbers JP17H05351 (Coordination Asymmetry), JP17K14455, JP18H01959, and Tokuyama Science Foundation.

Conflicts of interest

There are no conflicts to declare.

Notes and references

1 (a) S. Akine, S. Sunaga and T. Nabeshima, *Chem. Eur. J.*, 2011, **17**, 6853–6861; (b) Y. Liu, A. Singharoy, C. G. Mayne, A. Sengupta, K. Raghavachari, K. Schulten and A. H. Flood, *J. Am. Chem. Soc.*, 2016, **138**, 4843–4851; (c) T. Nakamura, G. Yamaguchi and T. Nabeshima, *Angew. Chem. Int. Ed.*, 2016, **55**, 9606–9609; (d) T. Okujima, C. Ando, S. Agrawal, H. Matsumoto, S. Mori, K. Ohara, I. Hisaki, T. Nakae, M. Takase, H. Uno and N. Kobayashi, *J. Am. Chem. Soc.*, 2016, **138**, 7540–7543; (e) M. Saikawa, T. Nakamura, J. Uchida, M. Yamamura and T. Nabeshima, *Chem. Commun.*, 2016, **52**, 10727–10730; (f) D. J. Kim, K. R. Hermann, A. Prokofjevs, M. T. Otley, C. Pezzato, M. Owczarek, J. F. Stoddart, *J. Am. Chem. Soc.*, 2017, **139**, 6635–6643; (g) P. Kumar and P. Venkatakrishnan, *Org. Lett.*, 2018, **20**, 1295–1299; (h) G. Anguera, W.-Y. Cha, M. D. Moore, J. Lee, S. Guo, V. M. Lynch, D. Kim and J. L. Sessler, *J. Am. Chem. Soc.*, 2018, **140**, 4028–4034; (i) W. Liu, A. G. Oliver and B. D. Smith, *J. Am. Chem. Soc.*, 2018, **140**, 6810–6813.

2 (a) M. Albrecht, O. Osetska, T. Abel, G. Haberhauer and E. Ziegler, *Beilstein J. Org. Chem.*, 2009, **5**, 78; (b) S. Perera, X. Li, M. Soler, A. Schultz, C. Wesdemiotis, C. N. Moorefield and G. R. Newkome, *Angew. Chem. Int. Ed.*, 2010, **49**, 6539–6544; (c) J. Setsune, M. Kawama and T. Nishinaka, *Tetrahedron Lett.*, 2011, **52**, 1773–1777; (d) S. Akine, D. Kusama and T. Nabeshima, *Tetrahedron Lett.*, 2013, **54**, 205–209; (e) R. Katoono, Y. Tanaka, K. Kusaka, K. Fujiwara and T. Suzuki, *J. Org. Chem.*, 2015, **80**, 7613–7625; (f) S. Akine, F. Utsuno, S. Piao, H. Orita, S. Tsuzuki and T. Nabeshima, *Inorg. Chem.*, 2016, **55**, 810–821; (g) J. Mendez-Arroyo, A. I. d'Aquino, A. B. Chinen, Y. D. Manraj and C. A. Mirkin, *J. Am. Chem. Soc.*, 2017, **139**, 1368–1371; (h) Y. Sakata, S. Kobayashi and S. Akine, *Chem.Commun.*, 2017, **53**, 6363–6366; (i) E. Lee, H. Ju, I.-H. Park, J. H. Jung, M. Ikeda, S. Kuwahara, Y. Habata and S. S. Lee, *J. Am. Chem. Soc.*, 2018, **140**, 9669–9677; (j) T. Tsukamoto, R. Sasahara, A. Muranaka, Y. Miura, Y. Suzuki, M. Kimura, S. Miyagawa, T. Kawasaki, N. Kobayashi, M. Uchiyama and Y. Tokunaga, *Org. Lett.*, 2018, **20**, 4745–4748; (k) G.-Y. Wu, L.-J. Chen, L. Xu, X.-L. Zhao and H.-B. Yang, *Coord. Chem. Rev.*, 2018, **369**, 39–75.

3 T. Nakamura, H. Ube and M. Shionoya, *Chem. Lett.*, 2013, **42**, 328–334.

4 T. Nakamura, Y. Kaneko, E. Nishibori and T. Nabeshima, *Nat. Commun.*, 2017, **8**, 129.

5 (a) A. Bacchi, M. Carcelli, C. Pelizzi, G. Pelizzi, P. Pelagatti and S. Ugolotti, *Eur. J. Inorg. Chem.*, 2002, 2179–2187; (b) N. Gómez-Blanco, J. J. Fernández, A. Fernández, D. Vázquez-García, M. López-Torres and J. M. Vila, *Eur. J. Inorg. Chem.*, 2009, 3071–3083; (c) A. Behnia, M. A. Fard, J. M. Blacquiere and R. J. Puddephatt, *Dalton Trans.*, 2018, **47**, 3538–3548.

6 (a) I. V. Shevchenko, A. Fischer, P. G. Jones and R. Schmutzler, *Chem. Ber.*, 1992, **125**, 1325–1332; (b) F. Huang, L. Ma, Y. Che, H. Jiang, X. Chen and Y. Wang, *J. Org. Chem.*, 2018, **83**, 733–739.

7 (a) C. Bazzicalupi, A. Bencini, A. Bianchi, V. Fusi, E. Garcia-España, C. Giorgi, J. M. Llinares, J. A. Ramirez and B. Valtancoli, *Inorg. Chem.*, 1999, **38**, 620–621; (b) K. Omoto, S. Tashiro, M. Kuritani and M. Shionoya, *J. Am. Chem. Soc.*, 2014, **136**, 17946–17949; (c) Q. Gan, T. K. Ronson, D. A. Vosburg, J. D. Thoburn and J. R. Nitschke, *J. Am. Chem. Soc.*, 2015, **137**, 1770–1773.

8 (a) M. R. Kember, A. J. P. White and C. K. Williams, *Inorg. Chem.*, 2009, **48**, 9535–9542; (b) D. Huang and R. H. Holm, *J. Am. Chem. Soc.*, 2010, **132**, 4693–4701; (c) S. Takano, D. Takeuchi, K. Osakada, N. Akamatsu and A. Shishido, *Angew. Chem. Int. Ed.*, 2014, **53**, 9246–9250.

